Preparation of 5-[^{131}I]iodotubercidin for the detection of adenosine kinase

Dirk Bier[1], Marcus Holschbach[1], Franziska Wedekind[2], Wiebke Sihver[3], Birte Drewes[1], Annette Schulze[1], Felix Neumaier[1,4], Bernd Neumaier[1,4], Andreas Bauer[2]*

Forschungszentrum Jülich GmbH, [1]Institute of Neuroscience and Medicine, Nuclear Chemistry (INM-5), [2]Molecular Organization of the Brain (INM-2), Wilhelm-Johnen-Straße, 52428 Jülich, [3]Helmholtz-Zentrum Dresden-Rossendorf, Institute of Radiopharmaceutical Cancer Research, Bautzner Landstraße 400, 01328 Dresden, [4]University of Cologne, Faculty of Medicine and University Hospital Cologne, Institute of Radiochemistry and Experimental Molecular Imaging, 50937 Cologne, Germany

[*]Corresponding author
Dirk Bier, Ph.D.
Institute of Neuroscience and Medicine, Nuclear Chemistry (INM-5)
Forschungszentrum Jülich GmbH
Tel: +49 2461 61 6330
Fax: +49 2461 61 2535
E-mail: d.bier@fz-juelich.de

Abstract

5-iodotubercidin is a prototype adenosine kinase (AK) inhibitor with potent anti-seizure activity in rodent epilepsy models. Using the chloramine-T method for radioiodination of tubercidin with ^{131}I, we prepared no-carrier-added 5-[^{131}I]iodotubercidin (5-[^{131}I]IT) in a radiochemical yield of 61 ± 13 % and with a radiochemical purity of >99 % (molar activity = 10 – 40 GBq/µmol). *In vitro* competition and saturation experiments demonstrated specific binding of 5-[^{131}I]IT in rodent brain slices (K_D~31 nM), but *ex vivo* autoradiography revealed its accumulation in cerebral vessels. We conclude that 5-[^{131}I]IT could be a useful tool for the detection and quantification of AK in *in vitro* studies.

Keywords

Nucleoside adenosine kinase inhibitor (AKI), n.c.a. radioiodination, iodotubercidin, in-vitro / ex vivo autoradiography

Introduction

The purine ribonucleoside adenosine (Ado) is a short-lived neuronal signaling molecule and metabolic regulator formed by intra- and extracellular breakdown of adenine nucleotides. Cerebral ischemia, epileptic seizures and traumatic brain injury lead to a dramatic increase of extracellular Ado that mediates feedback inhibition of excitatory activity and is supposed to be one of the mechanisms by which the brain protects itself from injury [1–5]. Ado is mainly metabolized by adenosine kinase (AK), an evolutionary conserved cytosolic phosphotransferase that catalyzes its conversion into adenosine monophosphate (AMP). Because cellular uptake of Ado is driven by a bidirectional facilitated diffusion transporter [5], inhibition of AK decreases reuptake and results in increased extracellular Ado concentrations [6–10]. AK inhibitors (AKIs) have been shown to exert a number of protective functions, making them candidate drugs for anti-inflammatory [11–13], anti-nociceptive [14–16] and anti-convulsive [6, 11, 14–18] therapy. 5-Iodotubercidin (5-IT) is a tubercidin analog and prototype of the ribonucleoside AKIs that suppresses AK by competing with Ado for binding to the enzyme [17, 19–21]. Other potent members of this group with different heterocyclic cores and/or substituents in the 5’-position of the deoxyribose residue are 5’-deoxy-5-iodotubercidin 1 (5’d-5-IT), a naturally occurring marine nucleoside with the same 7-deazaadenine core as in 5-IT 2 [9, 22], and 5’amino-5’deoxyadenosine 3, a synthetic compound in which the aglycon portion is formed by adenine [23] (**Fig. 1**). Another group of heterocyclic substituted cyclopentane analogs of nucleoside AKIs with improved metabolic stability is exemplified by A-134974 (**Fig. 1**), which is derived by replacement of the ribose with a cyclopentane carbocyclic ring and truncation of the 5’-methylene atom [19]. Finally, a number of orally active, non-nucleoside AKIs like the pyridopyrimidine ABT 702 5 (**Fig. 1**) have been described and shown to be effective *in vivo* [19]. Although 5-IT and other ribonucleoside AKIs showed potent anti-seizure activity in rodent epilepsy models [17, 19] they did not meet the safety and side-effect profile required for further drug development [18]. They could, however, serve as

radiolabeled probes to visualize the distribution of AK and to localize epileptic foci that have been shown to overexpress AK due to local astrogliosis in rodent models and human patients [24–26]. Radiolabeling of 5-IT with iodine-125 was previously achieved via isotope exchange in a melt of pivalic acid [27] or through halogen exchange reaction with 5-bromotubercidin [28], respectively. Here, we used electrophilic iodo-functionalization with iodine-131 at the 5-position of tubercidin (which is activated by electron delocalization) to prepare no-carrier-added (n.c.a.) 5-[^{131}I]iodotubercidin ([^{131}I]**2**) and evaluated its binding characteristics by *in vitro* and *ex vivo* autoradiography.

Experimental

1 Materials

Tubercidin, 5-iodotubercidin and chloramine T were purchased from Merck (Merck, Taufkirchen, Germany). ABT-702 was obtained from Tocris (Tocris Bioscience, Bristol, UK). A-134974 dihydrochloride hydrate was purchased from Sigma Aldrich (Sigma-Aldrich Chemie GmbH, Taufkirchen, Germany). Double concentrated pH 7.0 buffer tablets (2 tablets / 100 mL water) were supplied by Fluka (Fluka, Buchs, Switzerland). [^{131}I]Sodium iodide was obtained from Perkin Elmer (Part Number NEZ035A).

2 Animals

For *ex vivo* autoradiography, 2 − 6 months old female NMRI mice were purchased from Charles River Laboratories (Wilmington, MA), kept under a natural light / dark cycle and provided *ad libitum* access to food and water.

For the *in vitro* autoradiographic experiments brain slices from 3-6 months old Sprague-Dawley rats (competition experiments) or female NMRI mouse (saturation experiments) were also purchased from Charles River Laboratories and kept as described above. The regional government approved all procedures according to the German Law on the Protection of Animals (TierSchG; approval no. AZ9.93.2.10.35.07.244). Animal experiments were also approved by the Animal Research Committee of the Scientific and Technical Advisory Board of the Research Center Jülich, Germany.

3 Radiochemistry

Radioiodination of tubercidin with [^{131}I]NaI and chloramine T in aqueous solution afforded 5-[^{131}I]iodotubercidin as schematically outlined in scheme 1. To a 0.1 M NaOH solution of [^{131}I]NaI (typically 7 MBq) was added the equivalent volume of 0.1 M HCl and buffer pH 7 (50 µL) followed by the addition of a tubercidin stock solution (3.5 mg / mL in 50 % aqueous ethanol, 10 µL, 35 µg, 0.13 µmol). The reaction was started by the addition of an aqueous solution of chloramine T (4 mg / mL, 10 µL, 40 µg, 0.14 µmol)

and allowed to proceed for 3 min at ambient temperature. The reaction was quenched by the addition of acetic acid (10 µL) and HPLC eluent (methanol / water / acetic acid, 25 / 75 / 0.2, v / v / v, 100 µL).

Purification was carried out by reversed phase HPLC (Pump: Knauer (Berlin, Germany) Smartline 1000, UV-detector: Knauer Smartline 260, Radiodection: NaI(Tl) well-type scintillation detector, Column: Kromasil – 5RP18, 250 × 4,6 mm; Eluent: methanol/water/acetic acid, 25/75/0.2, v/v/v; Flowrate 1 mL/min; UV-detection at 280 nm).The product peak was assigned by on-line monitoring of the UV absorbance at 280 nm and radioactivity of the effluent. In the following, the capacity factors are used instead of the retention times. The capacity factor is symbolized by k' and is calculated as: $k' = (t_R - t_0)/t_0$, where t_R is the retention time of the peak, and t_0 is the dead time of the column. Using the system described above, k' values of tubercidin and 5-iodotubercidin were 0.2 and 1.9, respectively.

From the UV detector chromatogram, the area under the curve (AUC) of the peak corresponding to 5-[^{131}I]iodotubercidin was determined and converted to the number of moles of compound injected by means of a calibration curve.

The determined radioactivity value was then divided by the molar amount of 5-[^{131}I]iodotubercidin to obtain the molar activity.

In vitro assays used the radiotracer adjusted to specific (molar) activities in the range of 3.7 GBq / µmol.

4 Synthesis of the non-radioactive reference compound and analysis

10 µL Aqueous tubercidin solution (3 mg / mL), 30 µL buffer solution (pH7, Fluka) and 2.5 µL sodium iodide solution (2 mg/mL) were successively pipetted into a reaction vial. After the addition of 10 µL chloramine-T solution (3 mg /mL) the reaction was allowed to proceed for 5 minutes at room temperature. Aliquots of the solution and of a solution of commercial 5-IT were then analyzed by LCMS. For these measurements the outlet of the UV-DAD-detector was coupled via electrospray interface to a mass spectrometer (MSQ PlusTM, Thermo Electron Corporation San Jose, USA). Nebulizer gas pressure was 6 bar and desolvation temperature was 450 °C. Positive ion electrospray ionization was used. The sprayer and cone voltages were 3000 V and either 50 or 185 V,

respectively. Positive ion spectra were recorded over a m/z range of 70 – 400 at a scan time of 1 s. Xcalibur software (version 3.0) provided with the instrument was used for the analysis. The same chromatographic conditions as those used for separation of the radiolabeled product were chosen.

The obtained averaged MS spectra (Cone voltage 185 V) at the position of the peak of the reference substance (m/z (relative intensities)): 80.1 (12.4 %), 97.1 (3.6 %), 107.1 (100 %), 112.1 (4.2 %), 117.1 (22.5 %), 134.1 (57.67 %), 139.2 (5.5 %), 261.1 (63.0 %), 276.1 (5.3 %), 303.1(2.2 %), 308.0 (13,0 %), 393.1 (51.5 %) $[M+H]^+$) and that of the peak of the iodination product: 80.1 (14.26 %), 97.1 (2.25 %), 107.1 (100 %), 112.1 (4.1 %), 117.1 (25.15 %), 134.1 (60.72 %), 139.2 (5.54 %), 261.1 (66.28 %), 276.1 (6.25 %), 303.1 (2.53%), 308.0 (13.43 %), 393.1 (50.13 %) $[M+H]^+$ correspond to each other.

The retention times in this system for the reference substance and the reaction product were in both cases 4.69 minutes.

The local maxima measured in the diode array detector of the obtained UV spectra of the peaks of the reference substance and the peak from the reaction mixture were identical (203 nm, 238 nm and 285 nm).

5 In vitro stability

The product isolated after labeling was left in the HPLC eluent at ambient temperature for up to three days and then analyzed using the HPLC conditions described above.

6 In vitro autoradiography

6.1 Competition experiment

After the animals were sacrificed, whole brains were rapidly removed and immediately frozen at −80 °C until use. For autoradiography, the brain sections were warmed to -20 °C, cut into 20 µm thick horizontal sections (CM 3050, Leica AG Microsystems, Germany), mounted onto silica-coated object glasses (Laboroptik GmbH, Germany), dried on silica gel overnight at 4 °C, and stored at −80 °C until use.

On the day of the experiments, the sections were incubated for 45 min at room temperature in 50 mM Tris-HCl (pH 7.4) containing 2.31 kBq of 5-[^{131}I]iodotubercidin,

together or without either 5-IT, tubercidin or ABT-702 in final concentrations of 1 µM, 1 µM and 5 µM, respectively. Labeling was terminated by rinsing the sections twice in 50 mM Tris-HCl for 30 seconds at 4 °C and by dipping them into deionized water. After drying at 37 °C, the sections were placed on a phosphor imaging plate (Fuji). Exposure time was 45 minutes. Laser scanning of the plates employed a phosphor imager BAS 5000 (Fuji) controlled with software provided by the vendor (Version 2.11a, Raytest Isotopenmessgeräte, Germany). Using the advanced image analyzer program AIDA 3.10 (Raytest Isotopenmessgeräte, Germany) data from regions of interest (ROIs) were analyzed.

6.2 Saturation experiments

After the mouse were sacrificed, the brain was quickly removed, immediately frozen in 2-methylbutane, and stored at -80 °C until cryosectioning. Coronal brain sections (20-µm thickness) were prepared in a cryostat microtome (CM 3050, Leica), thaw-mounted onto silanized slides (Laboroptik GmbH, Germany), dried, and stored at −80 °C until use.

After a pre-incubation in buffer (50 mM Tris-HCl containing 1 mM $MgCl_2$; pH 7.4) for 15 min at 4 °C, the slides were incubated in labeling buffer containing 5-[^{131}I]iodotubercidin at 10 different concentrations. Additional slices were incubated in labeling buffer containing the same concentration of radioligand and 25 µM A-134974 4 to determine non-specific binding. After 30 min, the sections were removed from the labeling buffer, washed twice in normal buffer for 5 min at 4 °C, rinsed in deionized water and dried.

Data of the hippocampal ROIs are displayed in fmol / mg ww, as the gray values of the five standards correspond to the concentrations of 40.6, 13.5, 4.5, 1.5 and 0.5 pmol iodotubercidin in 1 g pig brain tissue.

For quantification, slices were co-exposed with in-house calibrated pig brain standards (with a known concentration of 5-[^{131}I]iodotubercidin and a thickness of 20 µm) and exposed to a coated phosphor imaging plate (Fuji BAS-MS 20 x 25, Fujifilm) for 15 min. The plate was laser-scanned with a phosphor imager (BAS 5000; Fuji). The image file was generated with BAS-Reader 3.14, and regions of interests (ROIs) were defined with the image analyzer software AIDA 4.13 (both Raytest Isotopenmessgeräte, Germany).

ROIs were examined for saturation behavior with GraphPad Prism version 4.00 for Windows (GraphPad Software, La Jolla California USA, www.graphpad.com).

7 Ex vivo autoradiography

About 110 kBq of 5-[^{131}I]iodotubercidin with a molar activity of 3.7 GBq / μmol in 50 μL saline were injected into the tail vains of female NMRI mice. Animals were killed by cervical dislocation 10 min after injection, and brains were removed immediately. Additionally, blood probes and thyroid glands were retained. Samples were weighed and radioactivity values were measured in a γ-counter (Auto-Gamma MINAXI 5000 Packard). Brains were rapidly frozen at −80 °C and cut into horizontal or sagittal sections (thickness, 40 μm) at −80 °C.

Results and discussion

1 Radiochemistry

The radioiodination of tubercidin under the described conditions (**Scheme 1**) was easily achieved at ambient temperature in a reaction time of three minutes. The radiochemical yield was 61 ± 13 % (n=8) and the radiochemical purity exceeded 96 %. The molar activity was determined by means of a calibration curve recorded with unlabeled 5-IT.

Obtained molar (specific) activities were in accordance with the manufacturer‘s specification of [^{131}I]sodium iodide, taking into account the storage period (15-63 GBq / µmol). This result confirms the complete chromatographic base-line separation of the product peak from all other possible by-products (**Fig. 2**). Chromatographic analysis of blank preparations containing all reagents except iodide did not show a peak with the retention time of 5-IT.

2 Product identification

The radioactive product peak of the reaction solution showed the same retention time as that observed for commercially available nonradioactive 5-IT. Furthermore, tubercidin was reacted with non-radioactive iodine using similar conditions as in the radioiodination reactions. The solution containing the raw product was analyzed by LC-MS. The peak at k’ = 1.8 showed an m/z value corresponding to the expected iodinated tubercidin. Additionally, MS studies were performed with a higher cone voltage, which leads to fragmentation even in a simple ESI source. The obtained fragmentation spectra of the synthesized compound and of commercial 5-IT were identical, as were the local maxima

of the averaged UV spectra over the respective peak range. In summary, these results confirmed that the radiolabeled compound is 5-[^{131}I]iodotubercidin.

3 In vitro autoradiography

3.1 Competition experiments

To determine the specificity of tracer binding, we performed *in vitro* autoradiography in the absence and presence of various competitors. **Fig. 3A** shows total binding obtained by incubating a rat brain slice in 5-[^{131}I]iodotubercidin alone. Binding of the tracer was observed in most brain regions, which was expected because in the adult CNS AK is mainly expressed in astrocytes, which are almost uniformly distributed throughout the brain [24, 29]. In addition, AK activity in both rat and human brain was reported to be high in hindbrain, pons and hypothalamus, intermediate in cerebellum, temporal and occipital cortex, and low in parietal and frontal cortex [30], which is in good agreement with the tracer distribution in the present study (**Fig. 3A**). Incubation of brain slices in the presence of 1 µM tubercidin (**Fig. 3B**), resulted in reduced tracer accumulation in most brain regions although substantial bindingwas still observed in the cerebellum. In contrast, an effective displacement of the radiotracer was observed in the presence of 1 µM of non-labeled 5-IT **2** (**Fig. 3C**) or 5 µM of the non-nucleoside AKI ABT-702 **5** (**Fig. 3D**). Based on these findings, binding of the radiotracer in *in vitro* autoradiography was mainly specific binding.

3.2 Saturation experiments

To confirm the specificity of the above findings, we performed a quantitative autoradiographic saturation study (**Fig. 4**). Non-specific binding, determined in the presence of 25 µM A-13497, increased linearly with increasing tracer concentrations, while specific binding, determined from the difference of total and non-specific binding, showed a clear saturation, providing evidence for a finite number of specific binding sites. The K_D value obtained by non-linear regression was 31 nM (95 % confidence interval 26-36 nM) which is in close agreement with the IC_{50} value of 26 nM previously determined for the inhibition of human and rat AK by non-labeled 5-IT [17, 20]. The B_{max} value that corresponds to the tissue concentration of AK was 447 fmol/mg tissue ww (95% confidence interval 420-474 fmol/mg tissue ww), showing that a single binding experiment can be used to determine the concentration of AK in a given tissue section.

4 Ex-vivo autoradiography

Intraperitoneal injection of 5-IT produced potent anti-seizure activity in rodent epilepsy models [17] suggesting that the compound could cross the blood-brain barrier. On the other hand, >99 % of 5-[^{125}I]iodotubercidin injected in mice was reportedly trapped in red blood cells (RBCs), effectively preventing its use for *in vivo* imaging [28]. This property was investigated in more detail in another animal experiment (4 mice). Ten minutes after injection of 5-[^{131}I]iodotubercidin (110 kBq) animals were killed and brains, thyroid glands and blood were immediately removed. Determination of radioactivity uptake of total brains showed a value of 0.3 % ID / g. However, the autoradiographs of the sliced brains revealed that the radioactivity was exclusively localized in the large vessels and not in the surrounding brain tissue, supporting the previous findings that 5-IT accumulates in RBCs (**Fig. 5**). Unfortunately, 5-IT does not penetrate the BBB which is illustrated by the discrepancy between region-specific binding found in the *in vitro* experiments on brain slices and the absence of specific binding in *ex vivo* animal studies.

Conclusions

5-[^{131}]Iodotubercidin can be obtained by simple electrophilic radioiodination in high radiochemical yields. The total preparation time is only 20 minutes due to fast labeling and HPLC purification. Based on the lack of accumulation in brain tissue after i.v. injection in mice, the tracer appears to be unsuitable for *in vivo* molecular imaging with PET or SPECT.

However, it can be used to visualize and quantify AK in *in vitro* autoradiographic studies.

Scheme 1

Synthesis of 5-[^{131}I]iodotubercidin ([^{131}I]**2**) by radioiodination of tubercidin

Fig. 1

Structure of nucleoside (**1**-**4**) and non-nucleoside (**5**) adenosine kinase inhibitors and their *in vitro* activity (IC_{50}) against human adenosine kinase according to McGaraughty et al. [19]. Purine numbering is exemplified for compound **1**

Fig. 2

Radio-HPLC chromatogram. Representative chromatogram of the reaction solution obtained by using a Kromasil 5RP18 column (250 mm x 4,6 mm) and methanol / water / acetic acid, 25 / 75 / 0.2, v / v / v, as eluent at a flow rate of 1 ml / min; UV trace, black; radioactive trace, gray

Fig. 3

In vitro autoradiography after incubation of 20 µm horizontal rat brain slices with 2.3 kBq/mL n.c.a. 5-[^{131}I]iodotubercidin alone (**A**) or after blocking with 1 µM tubercidin (**B**), 1 µM non-radioactive 5-iodotubercidin (**C**) or 5 µM ABT-702 (**D**). Numbers next to the color scale represent the corresponding relative activity units

Fig. 4

Quantitative autoradiographic *in vitro* saturation study with 5-[^{131}]iodotubercidin in mouse hippocampal slices. The binding of each concentration was studied on up to three coronal slices. Shown are total binding (dots), determined by incubation with 5-[^{131}I]iodotubercidin only, non-specific binding (crosses), determined after blocking with 25 µM A-134974, and specific binding (inverted triangles), calculated from the difference of total and non-specific binding. The K_D value obtained from the specific binding data was 31 nM (95% confidence interval 26-36 nM) and a maximum specific binding of 447 fmol / mg ww. Data are shown as mean ± standard deviation

Fig. 5

Two horizontal plane levels of *ex vivo* autoradiographs with 5-[^{131}]iodotubercidin. Mice were sacrificed by cervical dislocation 10 minutes after injection of the tracer. Brains were removed immediately and cut into 40 µm horizontal slices

Scheme 1

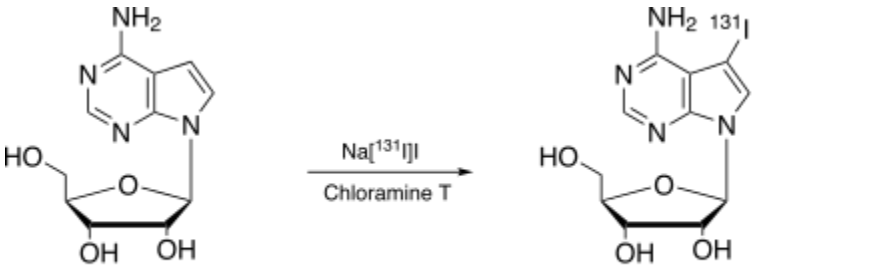

Tubercidin **4**

5-[^{131}I]iodotubercidin [^{131}I]**2**

Fig 1

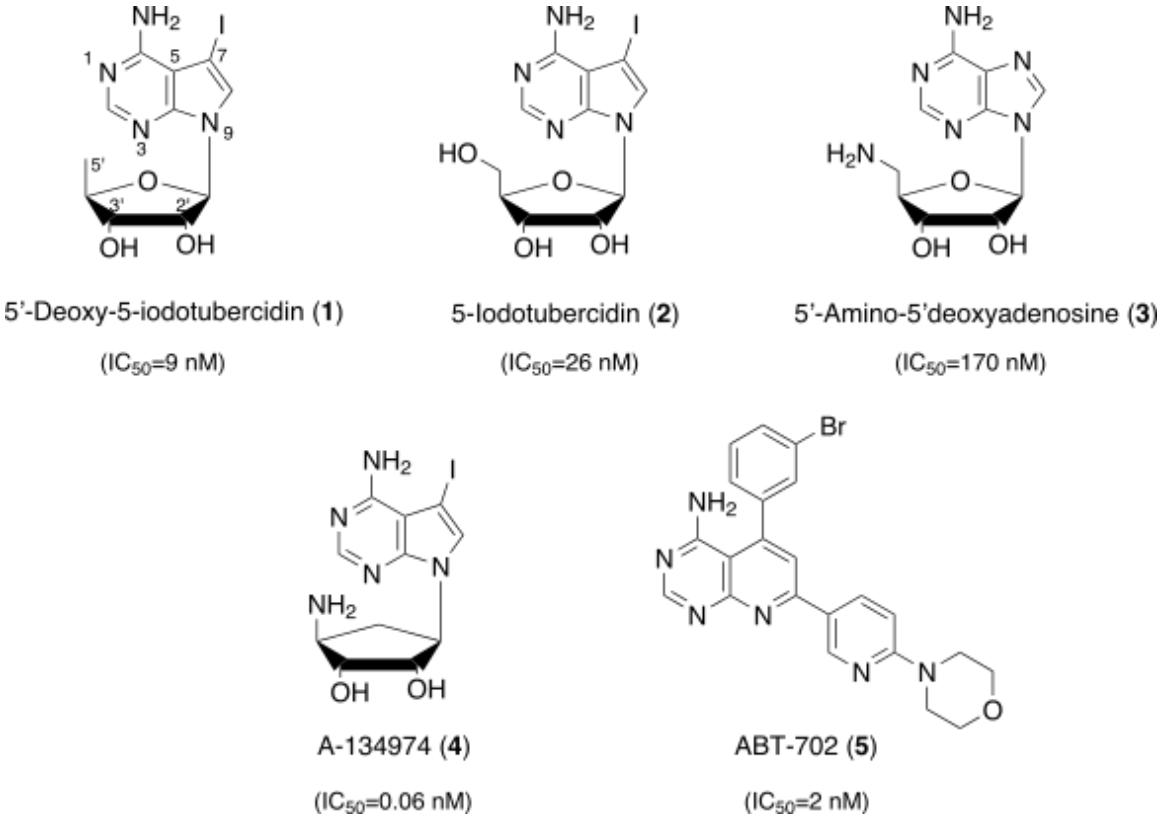

5'-Deoxy-5-iodotubercidin (**1**)

(IC_{50}=9 nM)

5-Iodotubercidin (**2**)

(IC_{50}=26 nM)

5'-Amino-5'deoxyadenosine (**3**)

(IC_{50}=170 nM)

A-134974 (**4**)

(IC_{50}=0.06 nM)

ABT-702 (**5**)

(IC_{50}=2 nM)

Fig 2

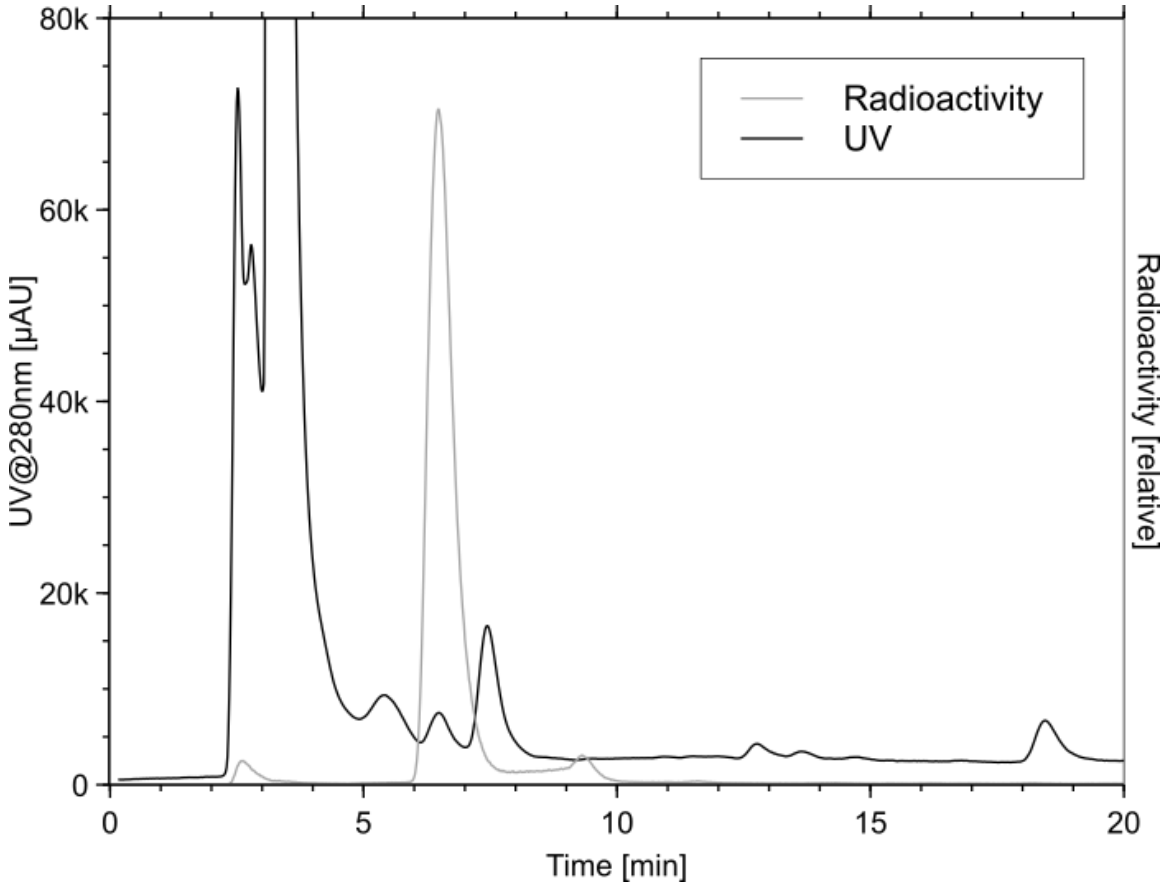
80k
60k
40k
20k
0
UV@280nm [µAU]
0
5
10
15
20
Time [min]
Radioactivity [relative]
Radioactivity
UV

Fig 3

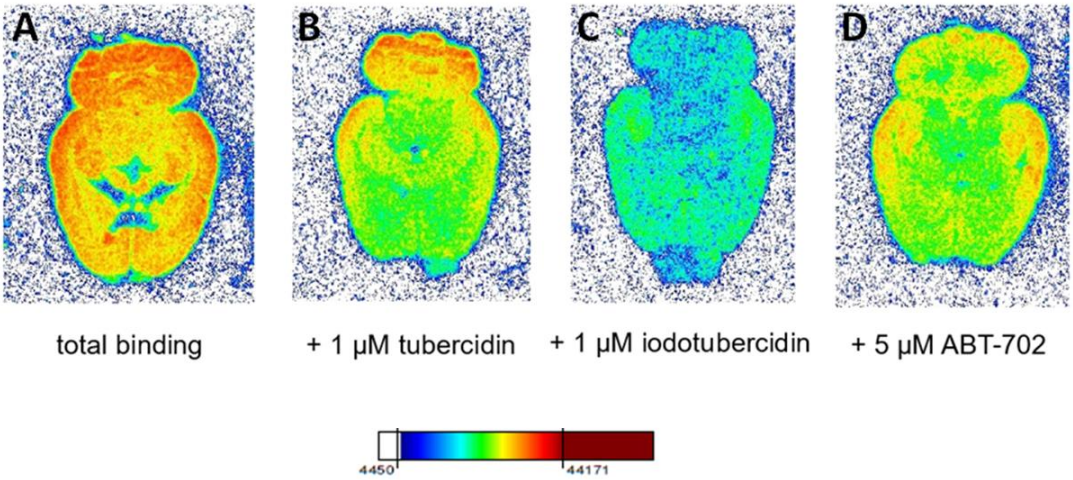
A
B
C
D
total binding
+ 1 µM tubercidin
+ 1 µM iodotubercidin
+ 5 µM ABT-702
4450
44171

Fig 4

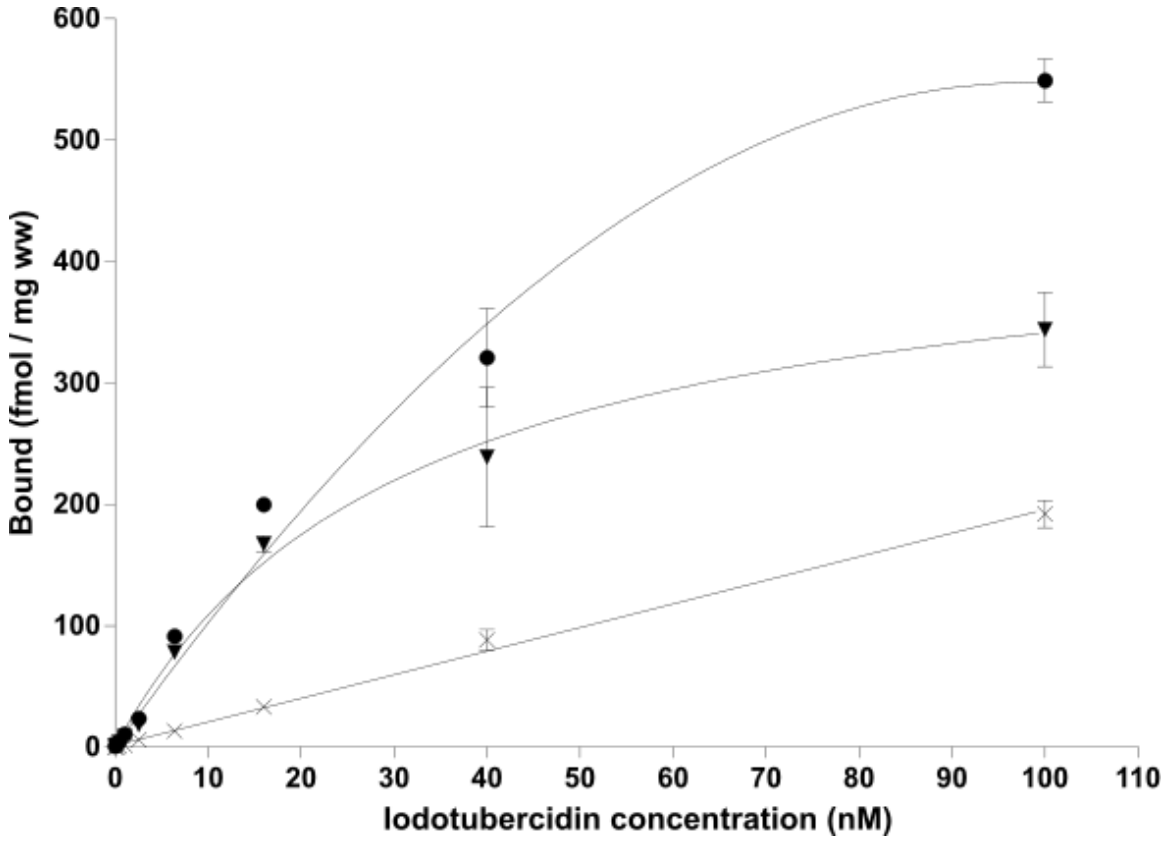
Bound (fmol / mg ww)
600
500
400
300
200
100
0
0
10
20
30
40
50
60
70
80
90
100
110
Iodotubercidin concentration (nM)

345 **Fig 5**

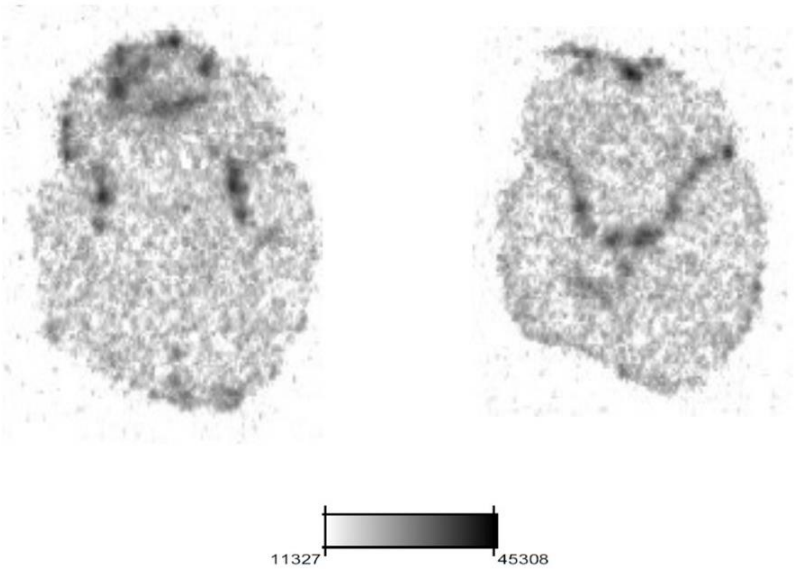

346

347

References

1. Berne RM, Rubio R, Curnish RR (1974) Release of adenosine from ischemic brain: effect on cerebral vascular resistance and incorporation into cerebral adenine nucleotides. Circulation Research 35(2):262–271

2. Ilie A, Raimondo JV, Akerman CJ (2012) Adenosine release during seizures attenuates GABAA receptor-mediated depolarization. Journal of Neuroscience 32(15):5321–5332

3. Pearson T, Damian K, Lynas RE, Frenguelli BG (2006) Sustained elevation of extracellular adenosine and activation of A1 receptors underlie the post-ischaemic inhibition of neuronal function in rat hippocampus in vitro. Journal of neurochemistry 97(5):1357–1368

4. Robertson CL, Bell MJ, Kochanek PM, Adelson PD, Ruppel RA, Carcillo JA, Wisniewski SR, Mi Z, Janesko KL, Clark RSB (2001) Increased adenosine in cerebrospinal fluid after severe traumatic brain injury in infants and children: association with severity of injury and excitotoxicity. Critical care medicine 29(12):2287–2293

5. Baldwin SA, Beal PR, Yao SYM, King AE, Cass CE, Young JD (2004) The equilibrative nucleoside transporter family, SLC29. Pflügers Archiv 447(5):735–743

6. Pak MA, Haas HL, Decking UKM, Schrader J (1994) Inhibition of adenosine kinase increases endogenous adenosine and depresses neuronal activity in hippocampal slices. Neuropharmacology 33(9):1049–1053

7. Golembiowska K, White TD, Sawynok J (1996) Adenosine kinase inhibitors augment release of adenosine from spinal cord slices. European journal of pharmacology 307(2):157–162

8. Liu XJ, White TD, Sawynok J (2000) Potentiation of formalin-evoked adenosine release by an adenosine kinase inhibitor and an adenosine deaminase inhibitor in the rat hind paw: a microdialysis study. European journal of pharmacology 408(2):143–152

9. Davies LP, Jamieson DD, Baird-Lambert JA, Kazlauskas R (1984) Halogenated pyrrolopyrimidine analogues of adenosine from marine organisms: pharmacological activities and potent inhibition of adenosine kinase. Biochemical pharmacology 33(3):347–355

10. Arch JRS, Newsholme EA (1978) Activities and some properties of 5′-nucleotidase, adenosine kinase and adenosine deaminase in tissues from vertebrates and invertebrates in relation to the control of the concentration and the physiological role of adenosine. Biochemical Journal 174(3):965–977

11. Ugarkar BG, Castellino AJ, DaRe JM, Kopcho JJ, Wiesner JB, Schanzer JM, Erion MD (2003) Adenosine kinase inhibitors. 2. Synthesis, enzyme inhibition, and antiseizure activity of diaryltubercidin analogues. Journal of medicinal chemistry 43(15):2894–2905

12. Firestein GS, Boyle D, Bullough DA, Gruber HE, Sajjadi FG, Montag A, Sambol B, Mullane KM (1994) Protective effect of an adenosine kinase inhibitor in septic shock. The Journal of Immunology 152(12):5853–5859

13. Firestein GS, Bullough DA, Erion MD, Jimenez R, Ramirez-Weinhouse M, Barankiewicz J, Smith CW, Gruber HE, Mullane KM (1995) Inhibition of neutrophil adhesion by adenosine and an adenosine kinase inhibitor. The role of selectins. The Journal of Immunology 154(1):326–334

14. Keil II GJ, DeLander GE (1994) Adenosine kinase and adenosine deaminase inhibition modulate spinal adenosine-and opioid agonist-induced antinociception in mice. European journal of pharmacology 271(1):37–46

15. Sawynok J, Liu XJ (2003) Adenosine in the spinal cord and periphery: release and regulation of pain. Progress in neurobiology 69(5):313–340

16. Jarvis MF, Yu H, Kohlhaas K, Alexander K, Lee C-H, Jiang M, Bhagwat SS, Williams M, Kowaluk EA (2000) ABT-702 (4-amino-5-(3-bromophenyl)-7-(6-morpholinopyridin-3-yl) pyrido [2, 3-d] pyrimidine), a novel orally effective adenosine kinase inhibitor with analgesic and anti-inflammatory properties: I. In vitro characterization and acute antinociceptive effects in the mouse. Journal of Pharmacology and Experimental Therapeutics 295(3):1156–1164

17. Ugarkar BG, DaRe JM, Kopcho JJ, Browne CE, Schanzer JM, Wiesner JB, Erion MD (2000) Adenosine kinase inhibitors. 1. Synthesis, enzyme inhibition, and antiseizure activity of 5-iodotubercidin analogues. Journal of medicinal chemistry 43(15):2883–2893

18. Wiesner JB, Ugarkar BG, Castellino AJ, Barankiewicz J, Dumas DP, Gruber HE, Foster AC, Erion MD (1999) Adenosine kinase inhibitors as a novel approach to anticonvulsant therapy. Journal of Pharmacology and Experimental Therapeutics 289(3):1669–1677

19. McGaraughty S, Cowart M, Jarvis MF (2006) Recent developments in the discovery of novel adenosine kinase inhibitors: mechanism of action and therapeutic potential. CNS drug reviews 7(4):415–432

20. Boison D (2013) Adenosine kinase: exploitation for therapeutic gain. Pharmacological reviews 65(3):906–943

21. Wotring LL, Townsend LB (1979) Study of the Cytotoxicity and Metabolism of 4-Amino-3-carboxamido-1-(β-d-ribofuranosyl) pyrazolo [3, 4-d] pyrimidine Using Inhibitors of Adenosine Kinase and Adenosine Deaminase. Cancer research 39(8):3018–3023

22. Mitchell SS, Pomerantz SC, Concepción GP, Ireland CM (1996) Tubercidin analogs from the ascidian Didemnum voeltzkowi. Journal of natural products 59(10):1000–1001

23. Miller RL, Adamczyk DL, Miller WH, Koszalka GW, Rideout JL, Beacham LM, Chao EY, Haggerty JJ, Krenitsky TA, Elion GB (1979) Adenosine kinase from rabbit

liver. II. Substrate and inhibitor specificity. Journal of Biological Chemistry 254(7):2346–2352

24. Gouder N, Scheurer L, Fritschy J-M, Boison D (2004) Overexpression of adenosine kinase in epileptic hippocampus contributes to epileptogenesis. Journal of Neuroscience 24(3):692–701

25. Aronica E, Zurolo E, Iyer A, Groot M de, Anink J, Carbonell C, van Vliet EA, Baayen JC, Boison D, Gorter JA (2011) Upregulation of adenosine kinase in astrocytes in experimental and human temporal lobe epilepsy. Epilepsia 52(9):1645–1655

26. Boison D (2008) The adenosine kinase hypothesis of epileptogenesis. Progress in neurobiology 84(3):249–262

27. Weichert JP, van Dort ME, Groziak MP, Counsell RE (1986) Radioiodination via isotope exchange in pivalic acid. International Journal of Radiation Applications and Instrumentation. Part A. Applied Radiation and Isotopes 37(8):907–913

28. Lohith K, Kwon S, Padakanti P, Lieberman B, Sandau U, Boison D, Mach R, Farwell M (2017) Synthesis and initial characterization of [125I]-5-iodotubercidin, a radioligand for imaging adenosine kinase. Journal of Nuclear Medicine 58(supplement 1):866

29. Studer FE, Fedele DE, Marowsky A, Schwerdel C, Wernli K, Vogt K, Fritschy JM, Boison D (2006) Shift of adenosine kinase expression from neurons to astrocytes during postnatal development suggests dual functionality of the enzyme. Neuroscience 142(1):125–137

30. Phillips E, Newsholme EA (1979) Maximum activities, properties and distribution of 5’nucleotidase, adenosine kinase and adenosine deaminase in rat and human brain. Journal of neurochemistry 33(2):553–558